

Review

Effect of Methane Adsorption on Mechanical Performance of Coal

Feng Cai ^{*,†} , Jingwen Yin [†] and Juqiang Feng [†] 

State Key Laboratory of Mining Response and Disaster Prevention and Control in Deep Coal Mines, Anhui University of Science and Technology, Huainan 232001, China; yjw1971228@163.com (J.Y.); fjq5060912@126.com (J.F.)

* Correspondence: fcgai@aust.edu.cn

† These authors contributed equally to this work.

Abstract: Understanding the influence of methane adsorption on coal mechanical properties is an important prerequisite for preventing coal mining and gas mining disasters. In the present research, meager coal and gas coal samples were obtained from Huaneng Yunnan Diandong Energy Co., Ltd. The triaxial compression tests were carried out under different methane adsorption equilibrium pressures and confining pressures. The influence laws of different factors on the mechanical properties of coal were analyzed. The results show that the triaxial stress-strain curve of adsorbed methane coal has similar morphology with that of non-adsorbed coal. Under the same confining pressure, the stress-strain curve morphology of coal before and after adsorbing methane is basically the same but the compressive strength of coal after adsorbing methane decreases. The greater the adsorption equilibrium pressure of methane, the smaller the compressive strength of coal. The change in the mechanical properties (compressive strength and elastic modulus) of coal caused by methane adsorption can be described by the Langmuir curve and the correlation coefficient is more than 0.99. Under any stress environment, high-rank coal shows greater strength and lower elastic modulus than low-rank coal, which is mainly due to the existence of a developed cleat system in high-rank coal that provides more conditions for methane adsorption. The research results provide important data-based support for the prevention of coal and gas outbursts.

Keywords: methane; adsorption; coal; compressive strength; infiltration; triaxial mechanics



Citation: Cai, F.; Yin, J.; Feng, J. Effect of Methane Adsorption on Mechanical Performance of Coal. *Appl. Sci.* **2022**, *12*, 6597. <https://doi.org/10.3390/app12136597>

Academic Editors: Zhizhen Zhang, Xiaomeng Shi, Xuewei Liu and Xiaoli Xu

Received: 26 May 2022

Accepted: 24 June 2022

Published: 29 June 2022

Publisher's Note: MDPI stays neutral with regard to jurisdictional claims in published maps and institutional affiliations.



Copyright: © 2022 by the authors. Licensee MDPI, Basel, Switzerland. This article is an open access article distributed under the terms and conditions of the Creative Commons Attribution (CC BY) license (<https://creativecommons.org/licenses/by/4.0/>).

1. Introduction

With increasing mining activities, underground mining is reaching deeper levels, which are settled on geological environments different from shallow coal mines [1]. Disturbance of land by mining breaks the stress and gas pressure equilibrium of the original rock in the coal reservoir. During the process of tunneling, large mining spaces along the goaf result in a significantly high pressure on the working face and surrounding rock of the roadway [2,3]. As the surrounding rock is simultaneously affected by the lateral support pressure of the adjacent working face [4,5], the pressure of the surrounding rock can increase to values up to 10 times more than those of the original rock stress [6–8]. Additionally, the stored gas can also present different gusher states. This phenomenon inevitably leads to the movement, deformation, and even destruction of gas-containing coal rock strata [9,10], thus promoting the occurrence of coal mine power disasters, such as rock burst and coal and gas outbursts [11], posing a serious threat to coal mine workers. In order to eliminate potential dangers and effectively prevent the occurrence of coal mine power disasters, it is necessary to understand the laws of deformation and failure in gas-containing coal rocks. It is particularly important to study the mechanical properties of gas-containing raw coal under high stress environments [12,13].

The mechanical behavior of gas-containing coal rock under constant triaxial stress conditions have been thoroughly investigated. Wang et al. [14] analyzed strength variation

and elastic modulus in gas media by measuring the triaxial compressive strength and deformation of more than 200 gas-containing coal samples with an in-house triaxial experimental device. Li et al. [15] applied a triaxial experiment to anthracite samples containing high amounts of gas to investigate the effects of axial pressure and lateral pressure on coal deformation and coal seam permeability. Kang et al. [16] performed triaxial compression experiments at different confining and gas pressures to investigate energy consumption and the seepage characteristics of coal samples during the compression process. By using the intrinsic time plasticity theory, Qiu et al. [17] established a constitutive relationship for the intrinsic time of gas-containing coal. In addition, some scholars have studied the effects of geological conditions [18,19], temperature [20,21], different loading and unloading conditions [22,23], effective confining pressure [24,25], and waste characterization [26] on the performance of gas-bearing coal.

As shown herein, previous researchers have mostly studied the triaxial compression mechanisms in coal rock containing gas under varying condition of stress, gas pressure, and temperature. However, there are few reports on the mechanical behavior of high-rank coal and medium-rank coal under high stress environments. By using the original coal samples obtained in the Qujing mining area, we applied three-dimensional stress to study changes in mechanical properties of raw coal containing methane at different effective confining pressures and methane pressures. The study presented herein provides a valuable reference for deep coal seam mining for the prevention and control of coal and gas disasters, especially during the application of deep coal seam fracturing technology in surface coalbed projects.

2. Materials and Methods

2.1. Instruments and Sample

In the present experiments, we selected the coal rock adsorption-penetration-triaxial mechanical coupling system developed by Anhui University of Technology (as shown in Figure 1). The system includes three subsystems:

- (1) The adsorption subsystem is comprised of a flow meter, positive pressure air pump, vacuum pump, pressure sensor, high-pressure gas steel cylinder, several pipelines, pipe valves, and pressure reducing valves, among others. This subsystem was used to inject gas into both ends of the installed coal sample at a constant temperature (the room temperature was controlled by air conditioning) and constant pressure (the gas pressure was controlled using metering pump controls) until adsorption equilibrium.
- (2) The mechanical testing subsystem includes a triaxial pressure chamber, pressure frame, deformation sensor, loading controller, and porous backing plate, among others. This subsystem was used to perform triaxial tests on the coal sample during gas adsorption equilibrium.
- (3) The data acquisition subsystem consists of an acquisition card and computer. This subsystem was used to collect sensor data.

In the present research, coal samples were obtained from the undisturbed lump coal of C3 coal seam (meager coal) and C2 coal seam (gas coal) at Huaneng Yunnan Diandong Energy Co., Ltd. (Qujing, China). The burial depth of C3 and C2 coal seams where the sampling point is located is 366 m and 397 m, respectively. In the process of sampling, lump coal more than 0.5 m away from the coal wall was taken. After taking out the coal sample, it was placed into a sealed tank to prevent the coal sample from absorbing water and being oxidized. According to the standard recommended by the International Society for Rock Mechanics, the coal samples were processed to obtain $\varnothing 50 \text{ mm} \times 100 \text{ mm}$ specimens. Considering the discreteness and effects of the mechanical properties of coal seam in different bedding directions, the bedding plane of coal was placed perpendicular to the axis during processing. Taking into account the effects of the heterogeneity of coal water content on metal adsorption, the coal sample was dried at a temperature of 55 °C for 24 h in order to reduce the effects of water on the adsorption deformation and mechanical properties of coal.

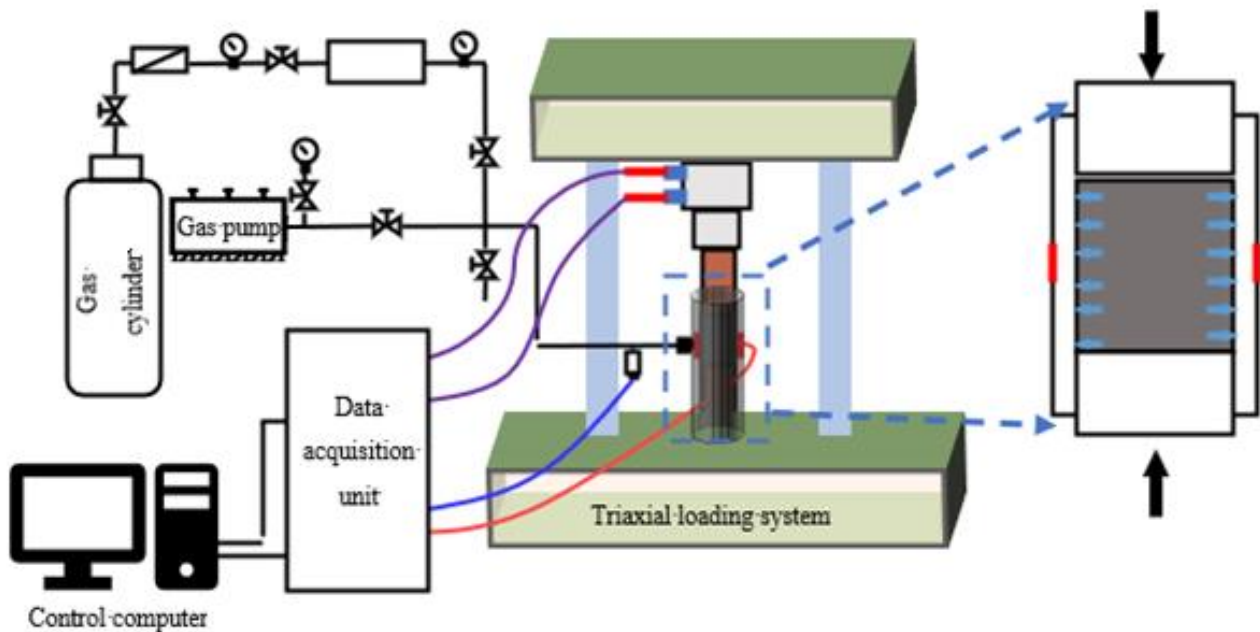


Figure 1. Structure diagram of test system.

2.2. Experimental Scheme

The mechanical characteristics of the raw coal-containing gas were determined using the triaxial compression test when the coal sample reached the gas adsorption equilibrium. Tests were performed at a constant confining and pore pressure. Axial loading was controlled by deformation and the deformation rate was 0.05 mm/min. Axial loading was applied until the failure limit of the coal sample was reached. During the test, gas pressure of coal samples was set to 1, 3, and 6 MPa, and confining pressure to 0, 3, 6, and 9 MPa. A total of 12 combined tests were carried out.

3. Results

Figures 2 and 3 show the stress-strain curves of coal samples under different combinations of confining and equilibrium pressure. As observed, each coal sample experienced four typical stages before reaching peak strength: (a) microfracture compression and closure; (b) elastic deformation; (c) stable fracture expansion; and (d) rapid fracture expansion.

At the initial stage, the external force compressed and closed the microfractures inside the sample, causing an increase in axial deformation. After the fracture completely closed, the increase in stress resulted in a linear variation of the axial and radial strain of the sample. That is, elastic deformation occurred. With a further increase in stress, internal fractures gradually appeared and steadily developed. When the stress was about to reach peak strength, the internal fracture expansion rate increased, the axial stress-strain curve did not show a yield point, the radial strain rate gradually increased, and finally the sample reached peak failure and entered the post-peak stage.

In the elastic stage, the slopes of the stress-strain curves in each subgraph were similar, the curve shapes were also relatively similar, and the peak stress variation of rock samples was less than 5%. These data indicates that the experimental method, process, and results obtained in the present research are reliable.

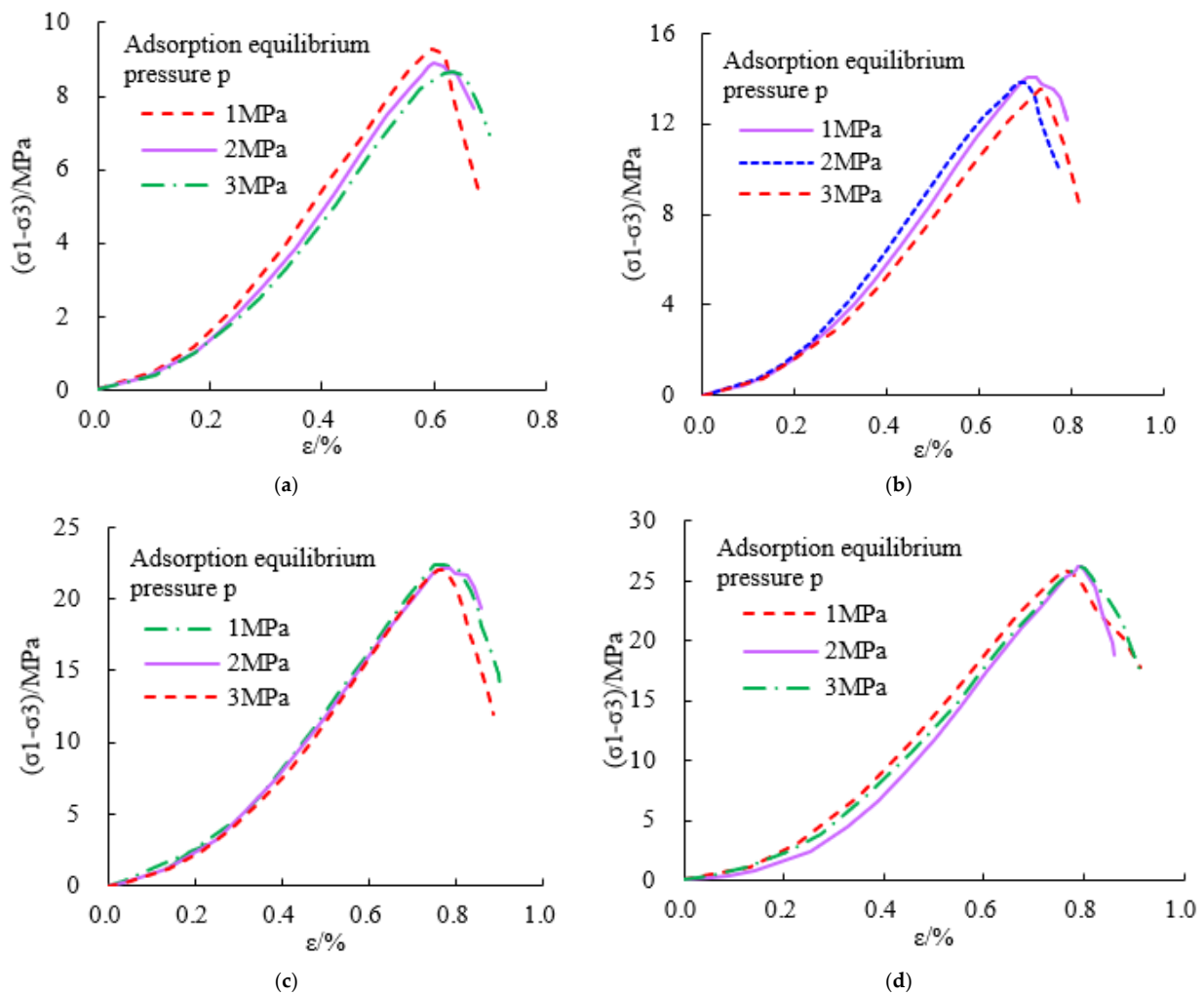


Figure 2. Meager coal triaxial compression stress-strain curve. (a) Stress-strain curve of Meager coal when confining pressure is 0 MPa. (b) Stress-strain curve of Meager coal when confining pressure is 3 MPa. (c) Stress-strain curve of Meager coal when confining pressure is 6 MPa. (d) Stress-strain curve of Meager coal when confining pressure is 9 MPa.

At a constant confining pressure, the shapes of the stress-strain curves of coal before and after methane adsorption were very similar. However, after methane adsorption, as the compressive strength of coal decreased, the equilibrium pressure for methane adsorption became higher and the compressive strength of coal became lower. When the adsorption equilibrium pressure was constant, the compressive strength, elastic modulus, and maximum strain of coal samples increased with the increase in confining pressure. In addition, when the confining pressure was constant, the compressive strength, elastic modulus, and maximum strain of coal samples decreased with the increase in confining pressure. As shown in Table 1, in meager coal, when the adsorption equilibrium pressure was 1 MPa and as the confining pressure increased from 0 to 3, 6, and 9 MPa, the compressive strength increased from 9.17 to 14.08, 22.38, and 26.21 MPa, respectively. Moreover, the elastic modulus increased from 1.98 to 2.59, 3.87, and 4.86 GPa, respectively. When the confining pressure was 3 MPa and the adsorption equilibrium pressure was 1 MPa, the amount of methane adsorbed was less than that observed at 2 and 3 MPa. Additionally, the compressive strength decreased from 14.08 to 13.87 and 13.61 MPa, respectively, and the elastic modulus from 2.59 to 2.41 and 2.29 GPa, correspondingly.

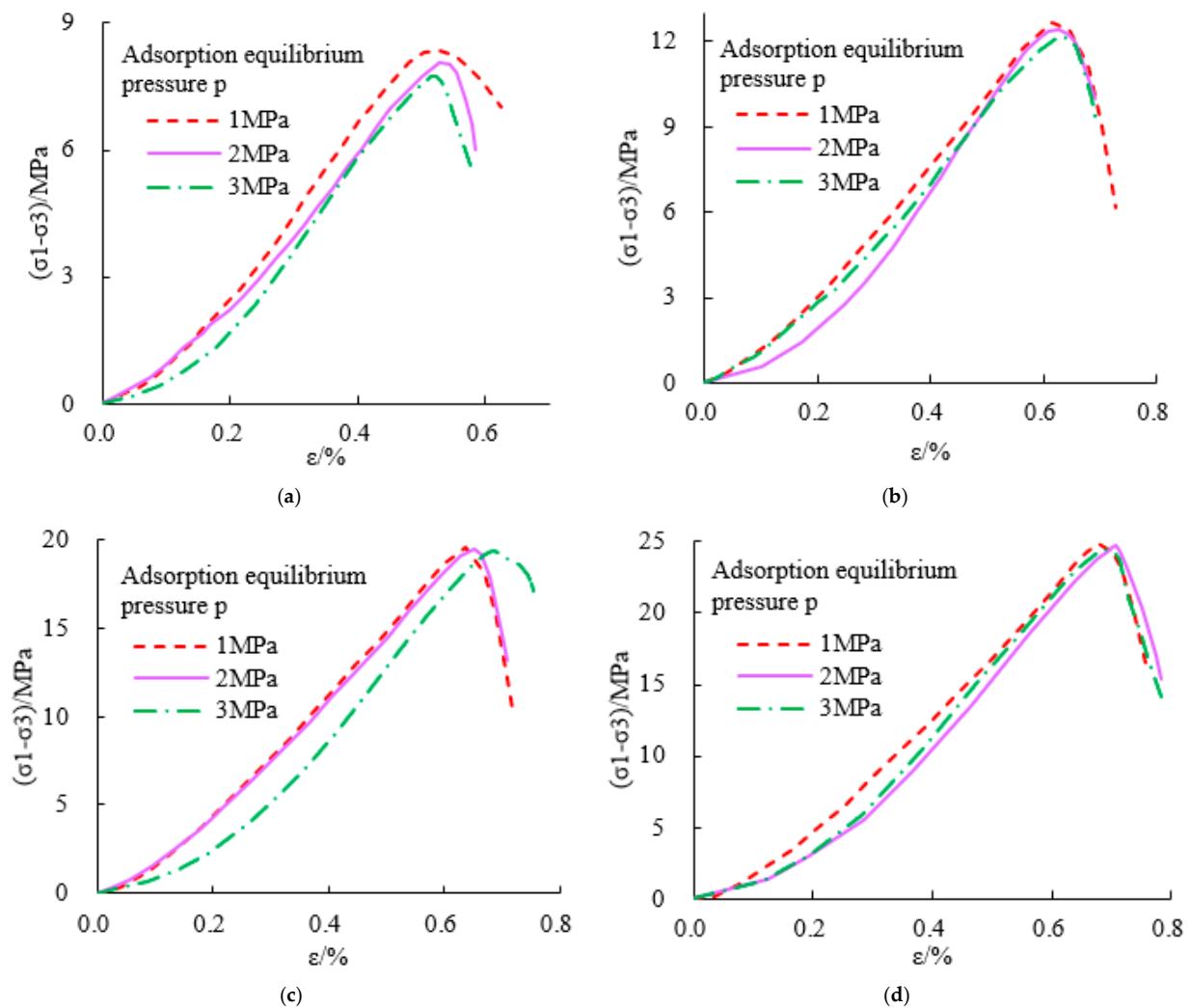


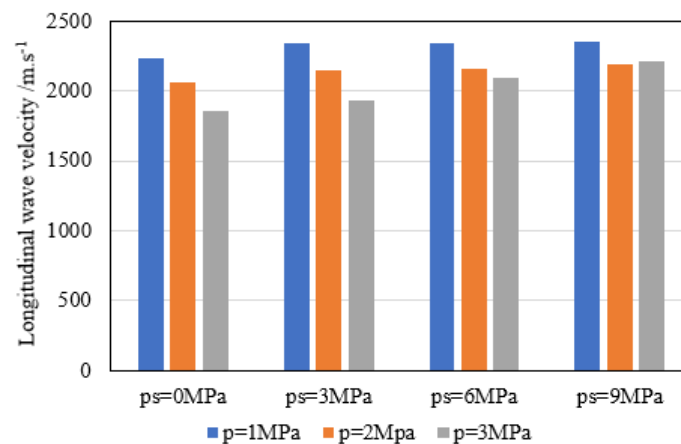
Figure 3. Gas coal triaxial compression stress-strain curve. (a) Stress-strain curve of Gas coal when confining pressure is 0 MPa. (b) Stress-strain curve of Gas coal when confining pressure is 3 MPa. (c) Stress-strain curve of Gas coal when confining pressure is 6 MPa. (d) Stress-strain curve of Gas coal when confining pressure is 9 MPa.

Table 1 shows the compressive strength σ_c and elastic modulus E of coal samples under different equilibrium pressures for methane adsorption. As shown in Table 1, under the same adsorption equilibrium pressure, the compressive strength and elastic modulus of meager coal were much larger than that of gas coal. In addition, the percentage of strength reduction for the meager coal after methane adsorption was higher than that observed in gas coal. The data in Table 1 shows that the elastic modulus of coal decreased with the increase in methane adsorption equilibrium pressure. This probably occurred because of the plastic effect of coal caused by methane adsorption. The plastic effect of coal occurs because the segmental mobility in the polymeric coal structure increases after methane adsorption. This produces coal softening, which weakens the structure of coal. Therefore, methane adsorption causes an expansion in coal volume, an increase in coal toughness, and a decrease in elastic modulus.

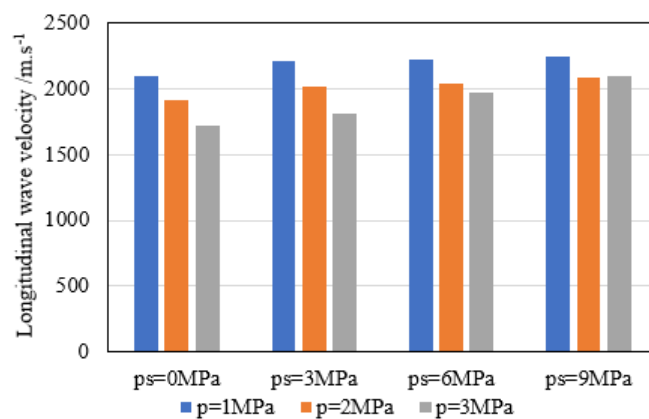
As shown in Table 1 and Figure 4, at a given adsorption equilibrium pressure and with the increase in confining pressure, the compression degree of the coal sample increased, as well as the longitudinal wave speed. On the contrary, at a constant confining pressure, the increase in adsorption equilibrium pressure resulted in an increase in the amount of methane adsorbed on coal. In addition, the coal volume expanded, which led to the continuous decrease in the longitudinal wave speed, which showed a variation of 10%.

Table 1. Experimental results.

Coal Quality	Adsorption Equilibrium Pressure p /MPa	Confining Pressure p_s /MPa	Compressive Strength σ_c /MPa	Modulus of Elasticity E /GPa	Longitudinal Wave Velocity/ $m.s^{-1}$
Meager coal	1	0	9.17	1.98	2238.943
		3	14.08	2.59	2338.796
		6	22.38	3.87	2342.136
		9	26.21	4.86	2350.827
	2	0	8.89	1.69	2056.944
		3	13.87	2.41	2151.145
		6	22.19	3.73	2154.296
		9	26.13	4.79	2190.796
	3	0	8.68	1.43	1858.014
		3	13.61	2.29	1933.194
		6	22.01	3.59	2090.706
		9	25.97	4.67	2210.848
Gas coal	1	0	8.36	1.69	2100.566
		3	12.65	2.18	2210.477
		6	19.62	3.78	2223.801
		9	24.85	4.39	2243.496
	2	0	8.03	1.33	1919.577
		3	12.41	1.97	2021.629
		6	19.50	3.58	2043.039
		9	24.71	4.26	2089.539
	3	0	7.69	1.19	1721.695
		3	12.17	1.71	1806.884
		6	19.38	3.35	1972.387
		9	24.56	4.13	2102.529



(a)



(b)

Figure 4. Longitudinal wave speed. (a) Meager coal. (b) Gas coal.

4. Discussion

4.1. Quantification of Coal Mechanical Parameters

Herein, the changes in the mechanical properties of coal caused by methane adsorption are expressed using a mathematical model [27]. After methane adsorption reached equilibrium, changes in the compressive strength of coal $\Delta\sigma_c$ increased with adsorption pressure, which can be expressed using the Langmuir equation [28]:

$$\Delta\sigma_c = \frac{\alpha p}{p + \beta} \tag{1}$$

where $\Delta\sigma_c$ represents the reduction in the compressive strength of coal caused by methane adsorption (MPa), p indicates methane adsorption equilibrium pressure (MPa), and α and β correspond to the curve fitting parameters.

Coal compressive strength after adsorption equilibrium of methane can be determined by:

$$\sigma_c = \sigma_0 - \Delta\sigma_c \tag{2}$$

where σ_0 is the compressive strength of the coal sample before methane adsorption in MPa.

Figure 5 shows the relationship between equilibrium pressure for methane adsorption and the reduction in coal compressive strength caused by methane adsorption. As shown in Figure 5, least square regression analysis indicates that meager coal and gas coal displayed R^2 values of 0.9983 and 0.9979, respectively. In addition, coal samples presented α values of 7.3217 and 0.3795, respectively, and β values of 5.9793 and 3.0916, correspondingly.

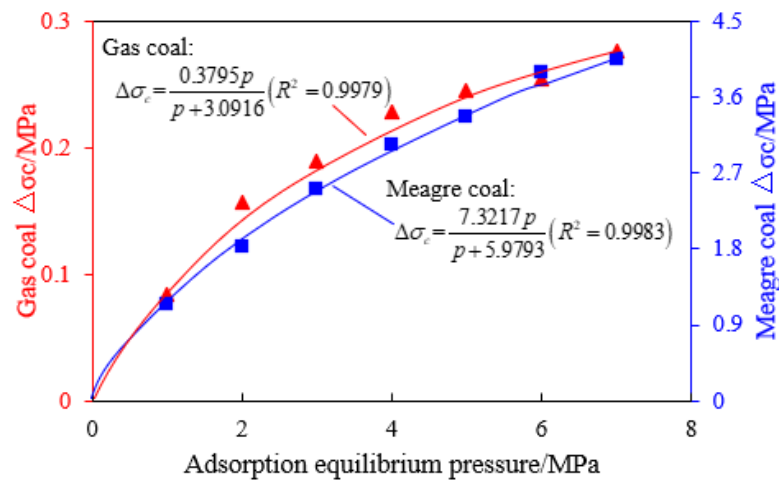


Figure 5. Reduction in compressive strength of coal sample vs. methane adsorption equilibrium pressure.

Reduction in the elastic modulus of coal caused by methane adsorption can be expressed as shown in Equation (3) and the elastic modulus of coal samples under different equilibrium pressures can be expressed by Equation (4), that is:

$$\Delta E = \frac{\lambda p}{p + \varphi} \tag{3}$$

$$E = E_0 - \Delta E \tag{4}$$

where ΔE represents the reduction in the elastic modulus of coal caused by methane adsorption (MPa), p is the equilibrium pressure for methane adsorption (MPa), λ and φ are the curve fitting parameters, and E_0 corresponds to the elastic modulus of coal before methane adsorption (MPa).

Figure 6 displays the relationship between equilibrium pressure for methane adsorption and elastic modulus reduction caused by methane adsorption on coal. In this case,

R^2 values for meager and gas coal were 0.9976 and 0.9991, respectively. The data also indicated λ values of 170.9973 and 9.9137, correspondingly, and φ values of 7.1612 and 2.0103, respectively.

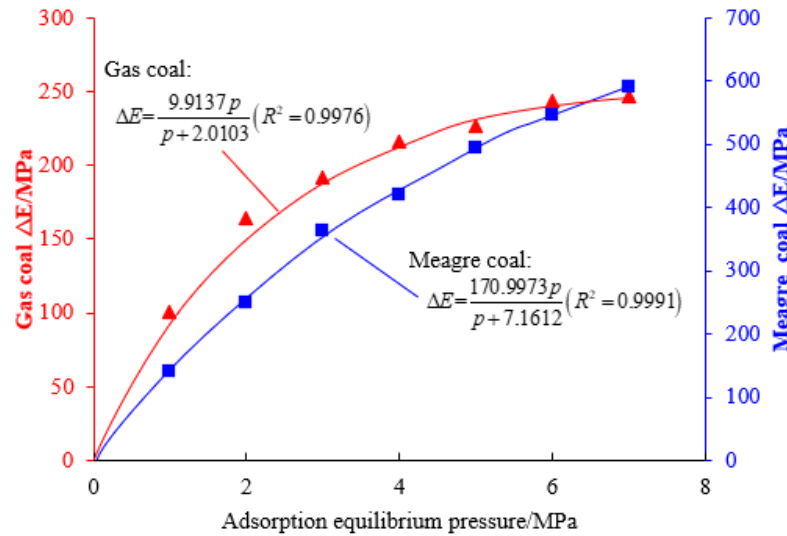


Figure 6. Reduction in elastic modulus vs. equilibrium pressure for methane adsorption.

In summary, the results obtained in these experiments were similar to those obtained using the Langmuir adsorption equation. Thus, we determined that the relationship between compressive strength reduction and the elastic modulus reduction for coal after methane adsorption and the adsorption equilibrium pressure depend on the experimental conditions and the metamorphic degree of coal.

4.2. Effects of Methane Adsorption on Tensile Strength of Coal

According to the results presented in Table 1, methane adsorption resulted in a significant reduction in coal compressive strength. This occurred because the structural reorganization and coal expansion caused after methane adsorption reduced the coal surface quality.

$$\Delta\gamma = -\frac{RT}{MS} \int_0^p Qd(\ln p) \tag{5}$$

where $\Delta\gamma$ is the surface energy variation (J), R is the ideal gas constant (8.314 J/mol·K), T corresponds to temperature (K), M indicates the molecular weight of methane, S represents the specific surface area of coal (m^2), Q is the adsorbed amount (mL/g), and p is the adsorption equilibrium pressure (MPa).

The tensile strength required to form a new fracture on coal surface is represented by:

$$\sigma = \sqrt{\frac{4\gamma E}{\pi L}} \tag{6}$$

where E is the elastic modulus of coal (MPa), γ corresponds to surface energy (J), and L indicates fracture length (mm).

Combination of Equations (5) and (6) result in the mathematical expression used to calculate the variation of tensile strength required to form a new fracture on coal samples during metal adsorption (Equation (7)):

$$\Delta\sigma = \sqrt{\frac{4ERT \int_0^p Qd(\ln p)}{MS\pi L}} \tag{7}$$

As shown in Equation (7), as equilibrium pressure for metal adsorption increases, surface energy decreases. This results in a reduction in coal strength and as a consequence,

a decrease in the tensile strength required to form coal fractures. When the pores and fissures in the gas-bearing coal increase, the elastic modulus and the stress at the critical inflection point of brittle ductile failure decrease. To produce the same strain, the axial stress required for the specimen with more gas content is lower. The distribution of pore and fissure content significantly reduces the ability of coal to resist deformation failure.

4.3. Effects of Metamorphic Degree of Coal on Compressive Strength

Figures 5 and 7 present the curve for the relationship between strength and elastic modulus reduction and adsorption equilibrium pressure in coal. Equations (1)–(4) were used to predict the compressive strength σ_c and elastic modulus E of coal samples under different equilibrium pressures for methane adsorption. As shown in Figure 7, in a triaxial stress environment and after methane adsorption, a more significant strength decrease was observed in high-rank coals as compared to low-rank coals. When equilibrium pressure for methane adsorption was 3.0 MPa, the compressive strength and elastic modulus of meager coal decreased by 14.91% and 19.67%, respectively. It was also observed that compressive strength and elastic modulus of gas coal decreased by 7.63% and 8.67%, correspondingly. When the equilibrium pressure for methane adsorption displayed a value of 6.0 MPa, the compressive strength and elastic modulus of meager coal decreased by 23.17% and 32.76%, respectively, while those of gas coal decreased by 10.9% and 11.29%, correspondingly. The natural coal cleat system that is formed during the process of coalification is much more developed in high-rank coals than in low-rank coals. Thus, gas coal and meager coal present low and high stiffness, respectively. For this reason, meager coal shows a larger expansion after methane adsorption, which in consequence can produce more structural changes in the coal matrix.

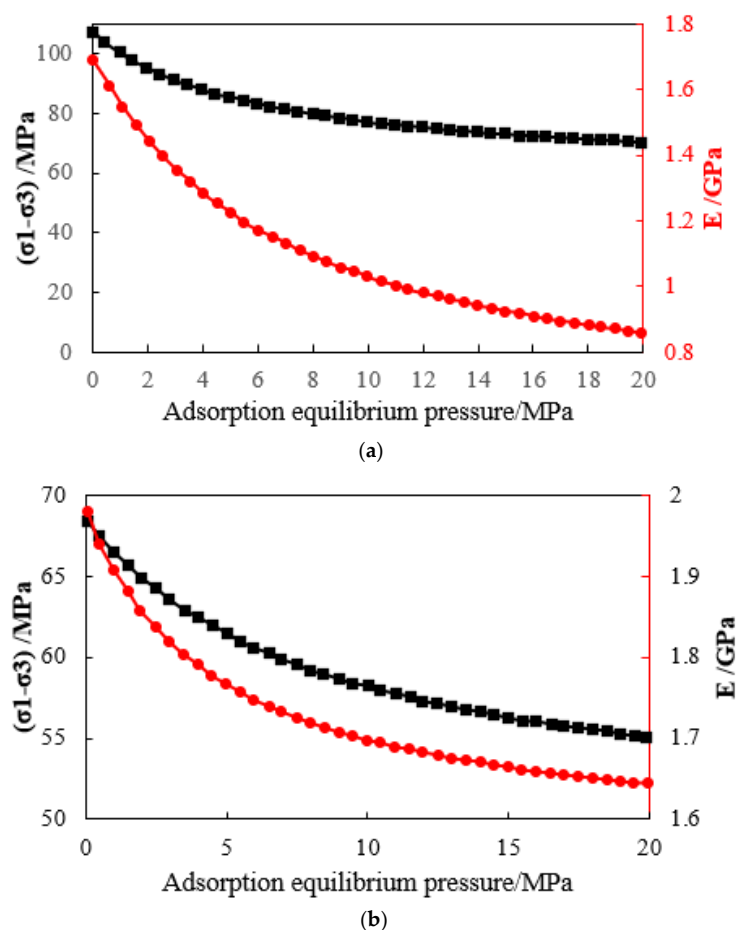


Figure 7. Prediction of compressive strength and elastic modulus of coal samples under different methane adsorption equilibrium pressures. (a) Lean coal. (b) Gas coal.

5. Conclusions

Triaxial compression tests were carried out under different methane adsorption equilibrium pressures and confining pressures. The main conclusions are as follows:

- (1) The triaxial stress-strain curve of a adsorbed methane coal body is similar to that of a non-adsorbed coal body, that is, before reaching the peak strength, it has gone through four typical stages: microfracture compression and closure, elastic deformation, stable fracture expansion, and rapid fracture expansion stage. However, the compressive strength of coal decreases after methane adsorption. The greater the adsorption equilibrium pressure of methane, the smaller the compressive strength of coal.
- (2) When the adsorption equilibrium pressure is constant, the compressive strength, elastic modulus, and maximum strain of coal samples increase with the increase in the confining pressure; when the confining pressure is constant, the compressive strength, elastic modulus, and maximum strain of coal samples decrease with the increase in the confining pressure. The adsorbed methane reduces the surface energy of coal and then reduces the overall strength of coal. The adsorption of methane leads to the plastic effect of coal and the decrease in the elastic modulus of coal.
- (3) The change in the mechanical properties (compressive strength and elastic modulus) of coal caused by methane adsorption can be described by the Langmuir curve and the correlation coefficient is more than 0.99. Under any stress environment, high-rank coal shows greater strength and lower elastic modulus than low-rank coal, which is mainly due to the existence of a developed cleat system in high-rank coal that provides more conditions for methane adsorption.

Author Contributions: Conceptualization, F.C. and J.Y.; methodology, F.C.; formal analysis, J.F.; investigation, F.C. and J.F.; data curation, F.C.; writing—original draft preparation, F.C.; writing—review and editing, J.Y.; visualization, F.C., J.Y. and J.F.; supervision, F.C., J.Y. and J.F.; project administration, F.C., J.Y. and J.F.; funding acquisition, F.C. All authors have read and agreed to the published version of the manuscript.

Funding: This research was financially supported by the scientific research project of “Study on key technology of coal and gas CO mining based on 110 working method retaining roadway along goaf in eastern Yunnan mining area (Grant No. HNKJ21-HF07)”, sponsored by China Huaneng Group Co., Ltd., and by the Collaborative Innovation Project of Anhui Universities (Grant No. GXXT-2020-057).

Data Availability Statement: The authors confirm that the data supporting the findings of this study are available within the article.

Acknowledgments: We appreciate the support from the State Key Laboratory of Mining Response and Disaster Prevention and Control in Deep Coal Mines, and China Huaneng Group Co., Ltd.

Conflicts of Interest: The authors declare no conflict of interest.

References

1. Nikoosokhan, S.; Vandamme, M.; Dangla, P. A poromechanical model for coal seams saturated with binary mixtures of CH₄ and CO₂. *J. Mech. Phys. Solids* **2014**, *71*, 97–111. [[CrossRef](#)]
2. Liu, R.; He, Y.; Zhao, Y.; Jiang, X.; Ren, S. Statistical analysis of acoustic emission in uniaxial compression of tectonic and non-tectonic coal. *Appl. Sci.* **2020**, *10*, 3555. [[CrossRef](#)]
3. Masoudian, S.; Airey, D.W.; El-Zein, A. Experimental investigations on the effect of CO₂ on mechanics of coal. *Int. J. Coal Geol.* **2014**, *128*, 12–23. [[CrossRef](#)]
4. Zhang, Z.; Zhang, R.; Cao, Z.; Gao, M.; Zhang, Y.; Xie, J. Mechanical behavior and permeability evolution of coal under different mining-induced stress conditions and gas pressure. *Energies* **2020**, *13*, 2677. [[CrossRef](#)]
5. Karacan, C.O. Heterogeneous sorption and swelling in a confined and stressed coal during CO₂ injection. *Energy Fuels* **2003**, *17*, 1595–1608. [[CrossRef](#)]
6. Potyondy, O.D. The bonded-particle model as a tool for rock mechanics research and application: Current trends and future directions. *Geosyst. Eng.* **2015**, *18*, 1–28. [[CrossRef](#)]
7. Jiang, C.; Liu, X.; Wang, W.; Wei, W.; Duan, M. Three-dimensional visualization of the evolution of pores and fractures in reservoir rocks under triaxial stress. *Powder Technol.* **2021**, *378*, 585–592. [[CrossRef](#)]

8. Isaka, B.A.; Ranjith, P.G.; Rathnaweera, T.D.; Perera, M.S.A.; Kumari, W.G.P. Influence of long-term operation of supercritical carbon dioxide based enhanced geothermal system on mineralogical and microstructurally-induced mechanical alteration of surrounding rock mass. *Renew. Energy* **2019**, *136*, 428–441. [[CrossRef](#)]
9. Xu, T.; Feng, G.; Shi, Y. On fluid-rock chemical interaction in CO₂-based geothermal systems. *J. Geochem. Explor.* **2014**, *144*, 179–193. [[CrossRef](#)]
10. Na, J.; Xu, T.; Yuan, Y.; Feng, B.; Tian, H.; Bao, X. An integrated study of fluid-rock interaction in a CO₂-based enhanced geothermal system: A case study of Songliao Basin, China. *Appl. Geochem.* **2015**, *59*, 166–177. [[CrossRef](#)]
11. Stephansson, O.; Tsang, C.F.; Kautsky, F. Foreword. Special issue for thermos-hydro-mechanical coupling in rock mechanics. *Int. J. Rock Mech. Min. Sci.* **2001**, *38*, 1–4. [[CrossRef](#)]
12. Cho, S.H.; Ogata, Y.J.; Kaneko, K. Strain-rate dependency of the dynamic tensile strength of rock. *INT J. Rock Mech. Min.* **2003**, *40*, 763–777. [[CrossRef](#)]
13. Perera, M.S.A.; Ranathunga, A.S.; Ranjith, P.G. Effect of coal rank on various fluid saturations creating mechanical property alterations using Australian coals. *Energies* **2016**, *9*, 440. [[CrossRef](#)]
14. Yongjia, W.; Mengtao, Z. The study of endochronic constitutive equations of coal effected by gas and the determining of parameters by experiment. *Acta Mech. Solida Sin.* **1996**, *17*, 229–234.
15. Li, X.; Yin, G.; Zhao, H.; Wang, W.Z.; Jing, X.F. Experimental study of mechanical properties of outburst coal containing gas under triaxial compression. *Chin. J. Rock Mech. Eng.* **2010**, *29*, 3350–3358.
16. Kang, X.-T.; Huang, G.; Song, Z.-I.; Deng, B.-Z.; Luo, J.-Y.; Zhang, X. Research on characteristics of energy dissipation and seepage of coal containing gas under triaxial compression. *Rock Soil Mech.* **2015**, *36*, 762–768.
17. Qiu, Z.Y.; Pan, Y.S.; Luo, H. Study on influence of effective confining pressure on acoustic emission signal in coal fracture. *J. Saf. Sci. Technol.* **2015**, *11*, 47–53.
18. Harpalani, S. Gas Flow through Stressed Coal. Ph.D. Thesis, University of California Berkeley, Berkeley, CA, USA, 1985.
19. Gawuga, J. Flow of Gas through Stressed Carboniferous Strata. Ph.D. Thesis, University of Nottingham, Nottingham, UK, 1979.
20. Xu, J.; Zhang, D.D.; Peng, S.J.; Liu, D.; Wang, L. Experimental research on influence of temperature on mechanical properties of coal containing methane. *Chin. J. Rock Mech. Eng.* **2011**, *30*, 2730–2735.
21. Jiang, X.U.; Bobo, L.; Ting, Z.H.O.U. Experimental study of deformation and energy evolution law of coal under cyclic loading. *Chin. J. Rock Mech. Eng.* **2014**, *33*, 3563–3572.
22. Yin, G.Z.; Wang, D.K.; Zhang, D.M.; Wang, W.Z. Test analysis of deformation characteristics and compressive strengths of two types of coal specimens containing gas. *Chin. J. Rock Mech. Eng.* **2009**, *28*, 410–417.
23. Lei, Z.; Zhang, Y.; Zhang, S.; Fu, L.; Hu, Z.; Yu, Z.; Li, L.; Zhou, J. Electricity generation from a three-horizontal-well enhanced geothermal system in the Qiabuqia geothermal field, China: Slickwater fracturing treatments for different reservoir scenarios. *Renew. Energy* **2020**, *145*, 65–83. [[CrossRef](#)]
24. Xia, M.; Zhou, K. Particle simulation of the failure process of brittle rock under triaxial compression. *Int. J. Miner. Metall. Mater.* **2010**, *17*, 507–513. [[CrossRef](#)]
25. Shen, N.; Zhang, Q.; Li, X.; Bai, B.; Hu, H. Effects of water and ScCO₂ injection on the mechanical properties of granite at high temperatures. *Adv. Civ. Eng.* **2020**, *2020*, 8838989. [[CrossRef](#)]
26. Saleem, M.; Blaisi, N.I.; Alshamrani, O.S.D.; Al-Barjis, A. Fundamental investigation of solid waste generation and disposal behaviour in higher education institute in the Kingdom of Saudi Arabia. *Indoor Built Environ.* **2018**, *28*, 1420326X1880485. [[CrossRef](#)]
27. Jiang, L.; Cheng, Y.; Han, Z.; Li, Q.; Gao, Q.; Yan, C. Effect of frost heave on internal structure and mechanical behavior of rock mass at low temperature. *J. Appl. Sci. Eng.* **2018**, *21*, 527–539.
28. Kumari, W.G.P.; Ranjith, P.G.; Perera, M.S.A.; Shao, S.; Chen, B.K.; Lashin, A.; Al Arifi, N.; Rathnaweera, T.D. Mechanical behaviour of Australian Strathbogie granite under in-situ stress and temperature conditions: An application to geothermal energy extraction. *Geothermics* **2017**, *65*, 44–59. [[CrossRef](#)]